

# Lorentz violation effects in asymmetric two brane models: a nonperturbative analysis

K. Farakos \*

Department of Physics, National Technical University of Athens  
Zografou Campus, 157 80 Athens, Greece

## Abstract

We consider the case of bulk photons in a Lorentz violating brane background, with an asymmetric warping between space and time warp factors. A perturbative analysis, in a previous work, gave an energy dependent phase (or group) velocity of light:  $V_{ph}(\omega) = V_{ph}(0) - C_G \omega^2$  ( $C_G > 0$ ), which was derived up to second order of time independent perturbation theory. In this paper, we go beyond the perturbative result and we study the nonperturbative behavior of the phase velocity for larger energies, by solving numerically an eigenvalue problem for the wave function of the zero mode (4D photon). In particular we see that  $V_{ph}(\omega)$  is in general a monotonically decreasing function which tends asymptotically to a final value  $V_{ph}(\infty)$ . We compare with the results of perturbation theory and we obtain a very good agreement in the range of small energies. We also present a wave function analysis and we see that in the nonperturbative sector of the theory (very high energies), the zero mode and the massive KK modes tend to decouple from matter localized on the TeV brane.

---

\*kfarakos@central.ntua.gr

# Contents

<b>1</b>	<b>Introduction</b>	<b>1</b>
<b>2</b>	<b>Asymmetric two brane models</b>	<b>3</b>
2.1	5D AdS-Reissner-Nordstrom black holes . . . . .	3
2.2	Junction conditions . . . . .	4
2.3	5D AdS-Reissner-Nordstrom Solution as a linearized perturbation around the Randall-Sundrum metric . . . . .	5
2.4	Bulk photons in asymmetric two brane models . . . . .	6
<b>3</b>	<b>Phase and group velocity of photons: a nonperturbative analysis and a comparison with perturbation theory</b>	<b>7</b>
<b>4</b>	<b>Wavefunction analysis</b>	<b>11</b>
4.1	Zero mode . . . . .	11
4.2	First KK excitation . . . . .	12
<b>5</b>	<b>Discussion</b>	<b>14</b>

## 1 Introduction

Lorentz symmetry is assumed to be an exact symmetry of nature. However, there are many exotic theories, mainly quantum gravity and string models, which predict Lorentz violating effects in the high energy limit, see [1] and references therein. Such an effect is an energy dependent velocity of photons, as in the context of quantum gravity models of space time foam, where the vacuum behaves like a medium with a nontrivial subluminous refractive index. Accordingly, different times of arrival are expected when photons with very high energies, which are emitted simultaneously from remote astrophysical sources, reach the detectors of current experiments. Note that there are recent experimental data of MAGIC and FERMI telescopes, which imply a time delay of more energetic photons in comparison against lower-energy ones. However, such a difference may also have a conventional astrophysical interpretation: for example, photons with different energies may be emitted not simultaneously at their sources.

Beyond quantum gravity models, an alternative mechanism which can produce a nontrivial vacuum refractive index based on brane models with an asymmetric space-time warping, was proposed. This mechanism was studied in [2] using time independent perturbation theory. Here we will study this mechanism in the nonperturbative regime, by solving numerically the eigenvalue problem for the wave function of the 4D photon. Such a study is useful for an analysis of extremely high energy cosmic phenomena in the context of asymmetric warp models. An example might be ultra high energy photons with energies higher than  $10^{19}$  eV.

Brane world models [3, 4, 5] are models with extra dimensions which are used by theorists in order to address the hierarchy problem. According to this scenario, standard model particles are assumed to be localized in a three dimensional brane (our world), while gravitons

can propagate in the multidimensional bulk. Beyond the ADD scenario [4, 5] where the extra dimensions are assumed to be large, brane models in which the bulk space time is warped have been also proposed [6, 7]. In the case of warped space-time, the extra dimensions could be: (1) finite, if a second parallel brane world lies at a finite bulk distance from our world [6] or (2) infinite, if our world is viewed as an isolated brane, embedded in an (infinite) bulk space [7]. The previously mentioned model with the two branes, is often called first Randall Sundrum model (RS1-model). Generalizations of the above generic models, including, for instance, bulk fields along the extra dimension(s) or higher-order curvature corrections, have been also considered, see for example Refs. [8, 9, 10, 11] and references therein.

We will adopt the following generic ansatz for the metric in five dimensions

$$ds^2 = -\alpha^2(z)dt^2 + \beta^2(z)d\mathbf{x}^2 + \gamma^2(z)dz^2 \quad (1)$$

where  $z$  parameterizes the extra dimension. In contrast to the RS-model where the space and time warp factors are equal, in models with an asymmetric warping we have in general  $\alpha(z) \neq \beta(z)$ . Thus, although the induced metric on the brane (localized at  $z = 0$  for example) is Lorentz invariant upon considering the case  $\alpha(0) = \beta(0)$ , the metric of Eq. (1) does not preserve 4D Lorentz invariance in the bulk since  $\alpha(z) \neq \beta(z)$  for  $z \neq 0$ . In such models Lorentz violation is due to bulk particles which can "feel" the difference between the space and time warp factors toward the extra dimension. In the standard brane-world scenario only gravitons are allowed to propagate in the bulk, hence, in the tree level, Lorentz violation effects are expected only in the gravitational sector. In Refs. [12, 13] specific asymmetric models predict a superluminous propagation of gravitons. However, since the detection of gravitons is still not an experimental fact, we cannot use this effect in order to set restrictions to asymmetric brane models.

As we have already mentioned, in Ref. [2] an asymmetric model where photons can freely move between two parallel branes in a 5D black hole background was considered. A perturbative analysis, of this model, gave an energy-dependent phase (or group) velocity of light:

$$V_{ph}(\omega) = V_{ph}(0) - C_G \omega^2 \quad (C_G > 0) \quad (2)$$

and

$$V_{gr}(\omega) = V_{gr}(0) - 3C_G \omega^2 \quad (3)$$

which was derived up to second order of time independent perturbation theory. Usually, in the conventional models the only bulk particles are the gravitons, but in the case of bulk photons which will be considered here we can set severe constraints to the free parameters of asymmetric models, see Ref. [2].

In this paper, we have examined the nonperturbative regime of the model in Ref. [2], by solving numerically an eigenvalue problem for the wave function of the zero mode (4D photon). We found that  $V_{ph}(\omega)$  is indeed given by the perturbative formula of Eq. (2) in the range of small energies, but there is an inflection point after which perturbation theory is not valid, then the phase velocity decreases monotonically with energy and tends asymptotically to a limiting value  $V_{ph}(\infty)$ .

In section 2 we introduce an asymmetric model with bulk photons, which consists of two branes in a 5D charged black hole background, and we examine in detail the corresponding junction conditions on the two branes. In section 3 we present the nonperturbative analysis

for the phase velocity and group velocity of 4D photon, while in section 4 we study the behavior of the wave function of the zero mode and the first KK excitation. Finally in section 5, we present our conclusions and we discuss our results in connection with the MAGIC experiment, and the recent severe restrictions of ultra high energy cosmic rays on quadratic dispersion relations for the velocity of light.

## 2 Asymmetric two brane models

### 2.1 5D AdS-Reissner-Nordstrom black holes

We consider an action which includes 5D gravity, a negative cosmological constant  $\Lambda$ , plus a bulk U(1) gauge field [12]:

$$S = \int d^5x \sqrt{g} \left( \frac{1}{16\pi G_5} (R^{(5)} - 2\Lambda) - \frac{1}{4} B^{MN} B_{MN} \right) + \int d^4x \sqrt{g_{(br)}^{(+)}} \mathcal{L}_m^{(+)} + \int d^4x \sqrt{g_{(br)}^{(-)}} \mathcal{L}_m^{(-)}, \quad (4)$$

where  $G_5$  is the five dimensional Newton constant, and  $B_{MN} = \partial_M H_N - \partial_N H_M$  is the field strength of the U(1) gauge field  $H_M$ , with  $M, N = 0, 1 \dots 4$ . The four-dimensional terms in the action correspond to matter fields localized on the two branes of the model, which are located at  $r = r_+$  and  $r = r_-$  ( $r_- < r_+$ ), and described by two *perfect fluids*, localized on the two branes, with energy momentum tensors

$$T_{(+)\mu}^\nu = \text{Diag}(-\rho_+, p_+, p_+, p_+) \delta(r - r_+) \quad (5)$$

$$T_{(-)\mu}^\nu = \text{Diag}(-\rho_-, p_-, p_-, p_-) \delta(r - r_-) \quad (6)$$

As we will see in section 2.2, these brane terms are necessary for the solution of Eqs. (9) and (10) below to satisfy the Israel junction conditions on the two branes.

The corresponding Einstein equations can be written as

$$G_{MN} + \Lambda g_{MN} = 8\pi G_5 \left( \frac{\sqrt{|g_{(br)}^{(+)}|}}{\sqrt{|g|}} T_{\mu\nu}^{(+)} \delta_M^\mu \delta_N^\nu + \frac{\sqrt{|g_{(br)}^{(-)}|}}{\sqrt{|g|}} T_{\mu\nu}^{(-)} \delta_M^\mu \delta_N^\nu + T_{MN}^{(B)} \right) \quad (7)$$

where the energy momentum tensor for the U(1) Gauge field is:

$$T_{MN}^{(B)} = B_{MP} B_N^P - \frac{1}{4} g_{MN} B_{PS} B^{PS} \quad (8)$$

For the metric of the black hole solution we make the ansatz

$$ds^2 = -h(r) dt^2 + \ell^{-2} r^2 d\Sigma^2 + h(r)^{-1} dr^2 \quad (9)$$

where  $d\Sigma^2 = d\sigma^2 + \sigma^2 d\Omega^2$  is the metric of the spatial 3-sections, which in our case are assumed to have zero curvature. Moreover,  $\ell$  is the AdS radius which is equal to  $\sqrt{-\frac{6}{\Lambda}}$ .

By solving the Einstein equations (7) we obtain:

$$h(r) = \frac{r^2}{\ell^2} - \frac{\mu}{r^2} + \frac{Q^2}{r^4} \quad (10)$$

where  $\mu$  is the mass (in units of the five dimensional Planck scale) and  $Q$  the charge of the 5D *AdS-Reissner-Nordstrom* black hole. This, of course, presupposes the existence of extra bulk matter, namely a point-like source with mass  $\mu$  and charge  $Q$ . Note that, in the case of nonzero charge  $Q$ , a non-vanishing component  $B_{0r}$  of the bulk field-strength tensor  $B_{MN}$ :

$$B_{0r} = \frac{\sqrt{6}}{\sqrt{8\pi G_5}} \frac{Q}{r^3}, \quad (11)$$

is necessary so that the solution satisfies the corresponding Einstein-Maxwell equations.

## 2.2 Junction conditions

We can use the 5D AdS-Reissner-Nordstrom black hole solution in order to construct two brane models. As a first step, we place two branes, one at the position  $r = r_+$  (Planck brane) and the other at the position  $r = r_-$  (TeV brane) (note that  $r_+ > r_-$ ). We next assume that for  $r < r_+$  the 5D metric is given by Eq. (9), while for  $r > r_+$  the metric is given by Eq. (9) upon the replacement  $r \leftrightarrow r_+^2/r$ . The metric which is obtained in this way is  $Z_2$ -symmetric upon the replacement  $r \leftrightarrow r_+^2/r$ , and the points  $r_+$  and  $r_-$  correspond to the fixed points of the orbifold structure of the model.

The next step is to glue the two independent slices of the metric by including two perfect fluid energy momentum tensors on both branes, see Eqs. (5) and (6) above. Then we have to satisfy the junction conditions at the positions  $r = r_+$  and  $r = r_-$  (four junction conditions). In Refs. [12, 13] the junction condition for the corresponding single brane model has been derived. If we apply it in our case we take:

$$6\sqrt{h(r_\pm)} = \pm k_5^2 \rho_\pm r_\pm, \quad 18h'(r_\pm) = -k_5^4(2 + 3\omega_\pm)\rho_\pm r_\pm \quad (12)$$

and after same algebra we obtain

$$\frac{\mu\ell^2}{3r_+^4} = (1 + \frac{\omega_+}{36}k_5^4\ell^2\rho_+^2) = (1 + \frac{\omega_-}{36}k_5^4\ell^2\rho_-^2)\epsilon^4 \quad (13)$$

$$\frac{Q^2\ell^2}{2r_+^6} = (1 + \frac{1 + 3\omega_+}{72}k_5^4\ell^2\rho_+^2) = (1 + \frac{1 + 3\omega_-}{72}k_5^4\ell^2\rho_-^2)\epsilon^6 \quad (14)$$

where  $k_5 = 8\pi G_5$ , and  $(\rho_+, \rho_-)$  and  $(p_+, p_-)$  are the energy densities and pressures on the Planck and the TeV brane correspondingly. The equations of state are parameterized as usual by:

$$\omega_+ = p_+/\rho_+, \quad \omega_- = p_-/\rho_- \quad (15)$$

Note that  $\rho_+ > 0$  (positive tension brane) and  $\rho_- < 0$  (negative tension brane). The parameter  $\epsilon$  is defined as:

$$\epsilon = \frac{r_-}{r_+} \quad (16)$$

In order to address the hierarchy problem, in a similar way with that of RS1-model, we have to choose a very large ratio  $\epsilon = 10^{-16}$ . Now, if we define the parameters

$$\bar{\rho}_+ = \frac{k_5^2\ell}{6}\rho_+, \quad \bar{\rho}_- = \frac{k_5^2\ell}{6}\rho_- \quad (17)$$

$$\bar{\mu} = \frac{\mu\ell^2}{3r_+^4}\epsilon^{-4}, \quad \bar{Q}^2 = \frac{Q^2\ell^2}{2r_+^6}\epsilon^{-6} \quad (18)$$

we obtain that

$$\bar{\mu} = (1 + \omega_+ \bar{\rho}_+^2) \epsilon^{-4} = (1 + \omega_- \bar{\rho}_-^2) \quad (19)$$

$$\bar{Q}^2 = (1 + \frac{1 + 3\omega_+}{2} \bar{\rho}_+^2) \epsilon^{-6} = (1 + \frac{1 + 3\omega_-}{2} \bar{\rho}_-^2) \quad (20)$$

In what follows we will consider that  $0 < \bar{\mu} \ll 1$  and  $0 < \bar{Q}^2 \ll 1$ , as our purpose is to construct two brane models that are described by asymmetric metrics which are linearized perturbations around the RS1 metric. See also Eq. (28) for the perturbation  $\delta h$  below. This implies that  $r_+$ , which is the radius that determines the position of the Planck brane in the bulk, is (comparatively) a very large quantity <sup>1</sup>. In particular, we have to satisfy both the inequalities  $r_+^2 \epsilon^2 \gg \sqrt{\mu \ell}$  and  $r_+^3 \epsilon^3 \gg Q \ell$ .

By solving Eqs. (19) and (20) (they are four algebraic equations) we find the energy densities:

$$\bar{\rho}_+^2 = 1 - 3\bar{\mu} \epsilon^4 + 2\bar{Q}^2 \epsilon^6 \quad (21)$$

$$\bar{\rho}_-^2 = 1 - 3\bar{\mu} + 2\bar{Q}^2 \quad (22)$$

and the equation of state parameters

$$w_+ = -1 - 2\bar{\mu} \epsilon^4 + 2\bar{Q}^2 \epsilon^6 \quad (23)$$

$$w_- = -1 - 2\bar{\mu} + 2\bar{Q}^2 \quad (24)$$

We see that the energy densities  $\bar{\rho}_+$ ,  $\bar{\rho}_-$  and the state factor parameters  $w_+$ ,  $w_-$  depend only on the constants  $\bar{\mu}$  and  $\bar{Q}^2$  and the hierarchy parameter  $\epsilon$ . Note that for  $\omega_+ = -1$  and  $\omega_- = 1$  we obtain the first RS-model.

The equation of state parameters should respect the null energy condition  $\omega > -1$ , hence if we demand  $\omega_+ \geq -1$  and  $\omega_- \geq -1$  we obtain the following constraint :

$$\bar{\mu} \leq \bar{Q}^2 \epsilon^2 \quad (25)$$

This equation means that we can choose the parameters  $\bar{\mu} (> 0)$  and  $\bar{Q}^2 (> 0)$  arbitrarily insofar as they satisfy the constraint of Eq. (25). Note that between the two branes there are no horizons as the parameters  $\bar{\mu}$  and  $\bar{Q}^2$  are assumed to be very small, and the positions  $r_+$  and  $r_-$  of the two branes are very large.

Finally, we would like to stress the fact that, although this problem has been considered previously in the literature, see Refs. [12, 13], the results for the energy densities (Eqs. (21) and (22)) and the state factors (Eqs. (23) and (24)) are presented for the first time in the present paper.

### 2.3 5D AdS-Reissner-Nordstrom Solution as a linearized perturbation around the Randall-Sundrum metric

To write the 5D AdS-Reissner-Nordstrom solution as a *linearized perturbation* around the RS metric, we perform the following change of variables  $r \rightarrow z(r)$  in Eq. (9):

$$\begin{aligned} r &= r_+ e^{-kz}, & \text{for } z > 0 \\ r &= r_+ e^{kz}, & \text{for } z < 0, \end{aligned} \quad (26)$$

---

<sup>1</sup>Also  $r_-$  is a very large quantity because  $\bar{\mu} = \frac{\mu \ell^2}{3r_-^4}$  and  $\bar{Q}^2 = \frac{Q^2 \ell^2}{2r_-^6}$  are assumed to be very small numbers.

If we rescale  $x_\mu \rightarrow \frac{r_\pm}{\ell} x_\mu$  ( $\mu = 0, \dots, 3$ ), we obtain:

$$ds^2 = -a^2(z)h(z)dt^2 + a^2(z)d\mathbf{x}^2 + h(z)^{-1}dz^2 \quad (27)$$

where  $a(z) = e^{-k|z|}$ , and  $k = \ell^{-1}$  is the inverse  $AdS_5$  radius. For the function  $h(z)$  we obtain:

$$h(z) = 1 - \delta h(z), \quad \delta h(z) = 3 \bar{\mu} \epsilon^4 e^{4k|z|} - 2 \bar{Q}^2 \epsilon^6 e^{6k|z|} \quad (28)$$

The positions of the branes which are located at  $r_+$  and  $r_- = r_+ \epsilon$  in the original coordinate system, are determined in the new coordinate system by the equations  $z = 0$  and  $z = z_c$  correspondingly, where  $\epsilon = e^{-kz_c}$  ( $r_c = z_c/\pi$  is radius of the compact extra dimension). Note that the large hierarchy  $\epsilon \sim 10^{-16}$  is achieved if we choose  $z_c \simeq 37$ . In addition, we will assume that  $|\delta h(z)| \ll 1$  in the interval  $0 < z < z_c$ , or equivalently we adopt that  $\delta h(z)$  is only a small perturbation around the RS-metric. We shall use the term Planck brane for the positive tension brane at the position  $z = 0$ , and the term TeV brane for the negative tension brane, at  $z_c$ .

## 2.4 Bulk photons in asymmetric two brane models

In this section we will study the case of a 5D massless  $U(1)$  gauge boson  $A_N$  in the background of an asymmetrically warped solution of the form of Eq. (27). We stress that the gauge field  $A_N$  must not be confused with the gauge field  $H_N$ , introduced in the previous section. As we will see later, we will identify the zero mode of  $A_N$  with the standard four dimensional photon. On the other hand  $H_N$  is an additional bulk field which does not interact with the charged particles on the brane. The equation of motion for  $A_N$  reads:

$$\frac{1}{\sqrt{g}} \partial_M (\sqrt{g} g^{MN} g^{RS} F_{NS}) = 0 , \quad (29)$$

with  $F_{NS} = \partial_N A_S - \partial_S A_N$ , and  $N, S = 0, 1, \dots, 5$ . In the background metric of Eq. (27), Eq. (29) gives:

$$-\partial_z (a^2(z)h(z)\partial_z A_j) - \nabla^2 A_j + \frac{1}{h(z)} \partial_0^2 A_j = 0, \quad j = 1, 2, 3 , \quad (30)$$

where we have assumed the Coulomb gauge condition:

$$\vec{\nabla} \cdot \vec{A} = 0, \quad A_0 = 0, \quad A_z = 0 , \quad (31)$$

which is suitable for the case of a Lorentz violating background. On setting in Eq. (29):

$$A_j(x, z) = e^{ip \cdot x} \chi_j(z), \quad p_\mu = (-\omega, \mathbf{p}) \quad (32)$$

we obtain

$$-\partial_z \left\{ a^2(z)h(z)\partial_z \chi \right\} + \left\{ \mathbf{p}^2 - \frac{\omega^2}{h(z)} \right\} \chi = 0 \quad (33)$$

where for brevity we have dropped the index  $j$  from  $\chi$ . Note that the *spectrum* of Eq. (33) is *discrete*, due to the orbifold boundary conditions [6],  $\chi'(0) = 0$  and  $\chi'(z_c) = 0$  (where the prime denotes a  $z$ -derivative).

We would like review here briefly the spectrum in the case of RS1-model ( $\delta h = 0$ ), which consist of a zero mode plus an infinite tower of massive KK modes. It suffices to mention that the nonzero eigenvalues are:

$$m_n^{(0)} = x_n k e^{-kz_c}, \quad n = 1, 2, 3, \dots \quad (34)$$

where  $x_n$  are the roots of the zeroth order Bessel function  $J_0(x_n) = 0$ . On adopting  $kz_c \sim 12$ , which is the standard choice in order to connect electroweak (ew) and Planck scales ( $M_P = e^{kz_c} m_{ew}$ ) in a RS framework [6], one obtains that:

$$m_n^{(0)} \sim \text{TeV}, \quad n = 1, 2, \dots \quad (35)$$

The corresponding eigenfunctions are:

$$\chi_0^{(0)} = \frac{1}{N_0}, \quad N_0 = \sqrt{z_c} \quad (36)$$

$$\chi_n^{(0)} = \frac{1}{N_n} e^{kz} J_1\left(\frac{m_n^{(0)}}{k} e^{kz}\right), \quad N_n = \frac{e^{kz_c}}{\sqrt{2k}} J_1(x_n) \quad (37)$$

where the coefficients  $N_0, N_n$  are defined by the normalization condition:

$$\int_0^{z_c} \chi_n^{(0)}(z) \chi_m^{(0)}(z) dz = \delta_{mn} \quad (38)$$

### 3 Phase and group velocity of photons: a nonperturbative analysis and a comparison with perturbation theory

If we introduce the dimensionless variable  $y = kz$  in Eq. (33) we obtain

$$\partial_y^2 \chi + \left\{ -2 + \frac{h'}{h} \right\} \partial_y \chi - \frac{1}{a^2 h} \left\{ \left(\frac{\mathbf{p}}{k}\right)^2 - \frac{1}{h} \left(\frac{\omega}{k}\right)^2 \right\} \chi = 0 \quad (39)$$

where

$$h(y) = 1 - \delta e^{4y} (3 \tilde{c}_a - 2 e^{2y}), \quad \delta = \bar{Q}^2 \epsilon^6, \quad \tilde{c}_a = \frac{\bar{\mu}}{\bar{Q}^2 \epsilon^2} \quad (40)$$

and the boundary conditions now read:

$$\chi'(0) = 0, \quad \chi'(kz_c) = 0 \quad (41)$$

Note that  $0 < \tilde{c}_a \leq 1$  if we demand the null energy condition to be satisfied, see section 2.2 and Eq. (25) above. We have also checked that the value of  $\tilde{c}_a$  has not a significant impact for our numerical analysis, hence in what follows we will assume that  $\tilde{c}_a = 1$ , which is the case where  $\omega_+ = -1$ , see Eq. (23) above. Now, it is convenient to introduce a new parameter

$$\Delta = \bar{Q}^2 = \delta \epsilon^{-6} \quad (42)$$

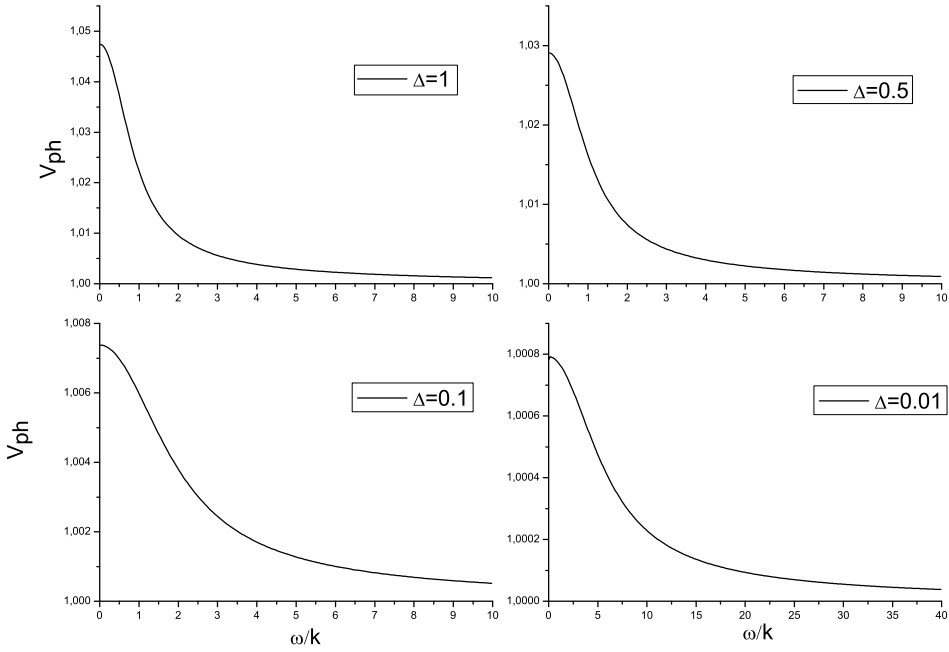


Figure 1: The phase velocity of the photon  $V_{ph}$  as function of  $\omega/k$  for  $kz_c = 2$  and  $\Delta = 1, 0.5, 0.1, 0.01$ . We see that as  $\Delta$  decreases the perturbative region of  $V_{ph}$  spreads towards larger energies  $\omega/k$ .

which can help us to estimate where perturbation theory fails as an approximation for solving Eq. (39). In particular, even for  $\Delta \ll 1$ , we can trust perturbation theory only if the energy of the photon  $\omega$  is relatively small. For larger energies  $\omega$  the term  ${}^2\omega^2\delta h$  ( $\delta h = 1 - h \simeq \Delta \ll 1$ ) in Eq. (33) (or in Eq. (39)) cannot be assumed small. In this case perturbation theory breaks down and a nonperturbative approach is necessary.

The nonperturbative analysis of this section is reduced to an eigenvalue problem of the second order differential equation (39) with the boundary conditions (41). We will consider that  $|\mathbf{p}|$  is fixed and will try to determine the energy  $\omega$  in order to satisfy the boundary conditions of Eq. (41). Note that there is an infinite tower of energies  $\omega_n$  ( $n=0,1,2..\right)$  which are solutions of the above mentioned eigenvalue problem for given momentum  $|\mathbf{p}|$ . The first eigenvalue  $\omega_0$  corresponds to the zero mode and the remaining eigenvalues  $\omega_n$  ( $n \neq 0$ ) to the massive KK excitations. Thus, we kept  $|\mathbf{p}|$  fixed and we integrated numerically <sup>3</sup>, for a number of values of  $\omega$  ( $\omega > |\mathbf{p}|$ ) separated by a relatively small constant step  $\delta\omega$ , Eq. (39) with the initial condition  $\chi(0) = 1$ ,  $\chi'(0) = 0$ . We observed that as we increased  $\omega$ ,

<sup>2</sup>We have used that  $h = 1 - \delta h$ , hence the term  $\frac{\omega^2}{h}$  in Eq. (33) can be written as  $\omega^2(1 + \delta h) = \omega^2 + \omega^2\delta h$ . The term  $\omega^2\delta h$  in the previous equation reveals the perturbative nature of Eq. 33 as  $\delta h \approx \Delta \ll 1$ . However, for large energies  $\omega \approx 1/\sqrt{\delta h}$  perturbation theory breaks down.

<sup>3</sup>For the numerical solving of the eigenvalue problem we have used mathematica programming.

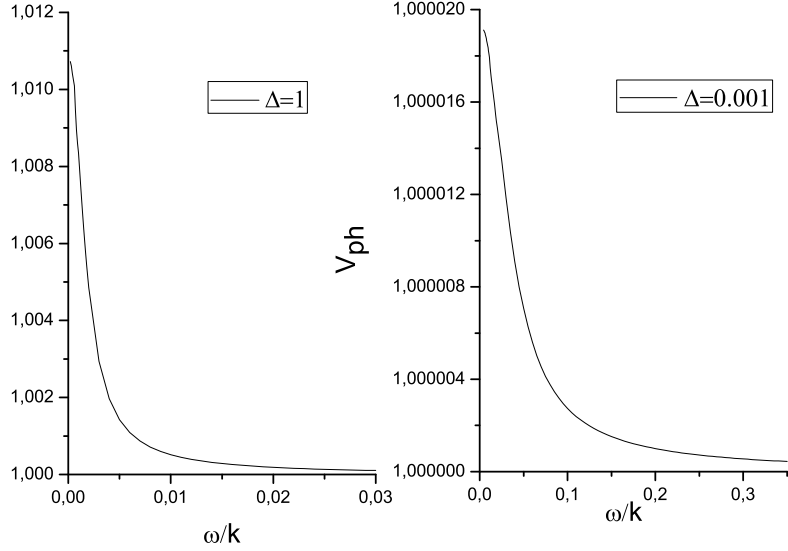


Figure 2: The phase velocity of the photon  $V_{ph}$  as function of  $\omega/k$  for  $kz_c = 8$  and  $\Delta = 1, 0.001$ . We see that even for larger hierarchies  $kz_c$  ( $\epsilon = e^{-kz_c}$ ) the qualitative features of the phase velocity do not change.

with the constant step  $\delta\omega$ , the derivative  $\chi'(kz_c)$  changed sign for first time (from positive to negative), in an interval of energies  $[\omega_a, \omega_a + \delta\omega]$ . In this interval the first eigenvalue  $\omega_0$  can be determined by bisection method. The infinite tower of energies  $\omega_n$  ( $n \neq 0$ ), can be determined in the same way.

The phase velocity

$$V_{ph} = \omega/|\mathbf{p}| \quad (43)$$

of the photon (zero mode) as a function of  $\omega$  (measured in units of  $k$ ) has been plotted in Fig.1, Fig.2 and Fig.3, for several values of  $\Delta$  and  $kz_c$  ( $\epsilon = e^{-kz_c}$ ). As we see, the phase velocity is a monotonically decreasing function which tends asymptotically to a constant value, seemingly equal to one independently from the parameters  $\Delta$  and  $kz_c$ .

In Fig. 4 we have plotted the group and phase velocity as a function of  $\omega/k$

$$V_{gr} = \frac{d\omega}{d|\mathbf{p}|} \quad (44)$$

We can observe that they have a very similar behavior. However, in contrast with the phase velocity, the group velocity becomes smaller than unity, then it increases and tends rapidly to unity. Also, as we see in Fig. 4, the phase and the group velocity are equal in the low energy limit as it is expected. It is well known that the phase and group velocity in vacuum should be identical, however for larger energies we observe significant differences because the vacuum behaves as a medium with a non-trivial refractive index. The perturbative formulas for the phase and group velocity, of Eqs. (2) and (3), agree with our numerical analysis in the low energy limit, as they give the same value for the group and phase velocity

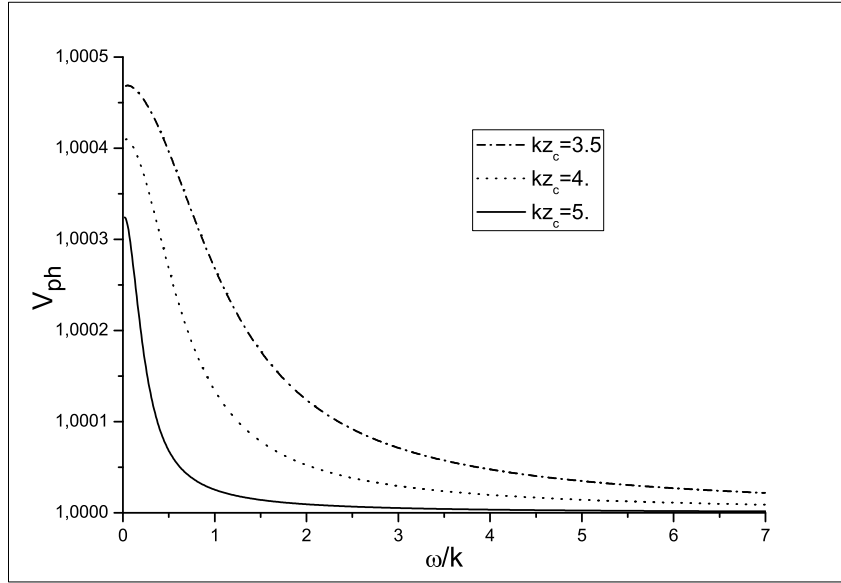


Figure 3: The phase velocity of the photon  $V_{ph}$  as function of  $\omega/k$  for  $kz_c = 3.5, 4, 5$  and  $\Delta = 0.01$ . As  $kz_c$  increases the perturbative region shrinks in the low energy range  $\omega/k \ll 1$ , and as a result the velocity  $V_{ph}$  tends to its limiting value in a much faster way.

for zero energy, decreasing quadratically with energy, while for larger energies outside the perturbative region they behave differently.

Especially in Fig.5, we observe that there is an inflexion point  $\omega_f$  which separates the perturbative from the nonperturbative sector of the theory. In the perturbative sector ( $\omega < \omega_f$ ) we expect that

$$V_{ph}(\omega) = V_{ph}(0) - C_G \omega^2, \quad (C_G > 0) \quad (45)$$

This formula has been derived in Ref. [2] by using second order time independent perturbation theory. The parameters  $V_{ph}(0)$  and  $C_G$  are given by the formulas of Eqs. (2.30) and (2.31) in [2]. These formulas are suitable for numerical computations, if the parameters  $\Delta$  and  $kz_c$  are known.

We also see, in Fig.5, that when  $\omega$  crosses the inflexion point  $\omega_f$  the rate of decreasing of the phase velocity gets smaller and the phase velocity possesses an asymptotic value equal to one. Note also, that the perturbative range of the phase velocity increases (or the inflexion point  $\omega_f$  is displaced towards the right direction in the figures) for smaller values of the parameter  $\Delta$ , as we see in Fig.1 and Fig.2.

At this point, we would like to stress that our numerical analysis is restricted to an unrealistic range of the parameter space of  $\Delta$  and  $kz_c$ , which is far beyond the physically interesting case of  $kz_c \simeq 37$ . However, it is reasonable that we are not in position to perform numerical computations in this case, as it demands great accuracy. This is mainly due to the extremely large values of the exponential  $e^{6kz}$ , that appear in Eq. (28).

Now, if we compare Fig.1 for  $kz_c = 2$  and Fig.2 for  $kz_c = 8$ , we see that the qualitative features of the phase velocity as a function of  $\omega$  are unchanged, although there is a significant

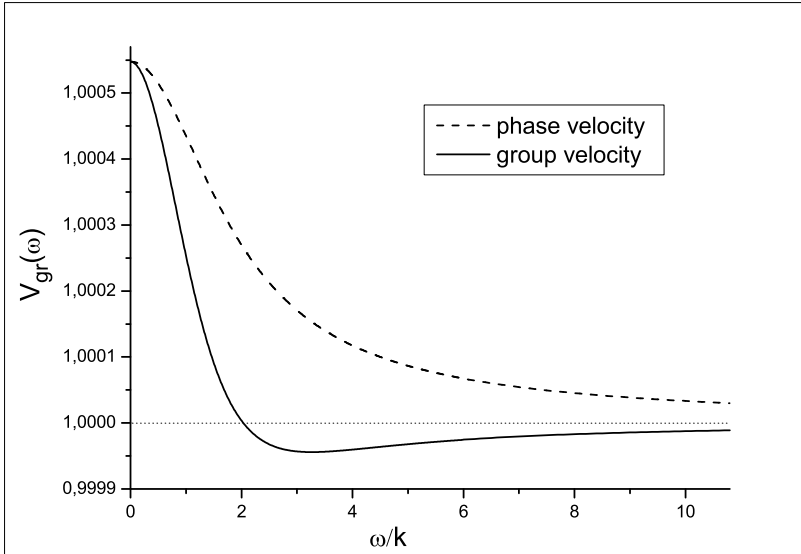


Figure 4: The phase and the group velocity of the photon ( $V_{ph}$  and  $V_{group}$  correspondingly) as a function of  $\omega/k$  for  $kz_c = 3$  and  $\Delta = 0.01$ .

difference between the corresponding hierarchies  $\epsilon_1 = e^{-2} \sim 10^{-1}$  and  $\epsilon_2 = e^{-8} \sim 10^{-4}$ . We have also performed computations for larger  $kz_c = 10$  ( $\epsilon_3 \sim 10^{-5}$ ) and we have confirmed the same behavior for the phase velocity. We also see that this behavior is independent from the parameter  $\Delta$ , which determines the perturbative range of our model. Accordingly, in the conclusions we will consider an extrapolation assuming that the qualitative behavior of the phase velocity is also valid for  $\epsilon \sim 10^{-16}$  which is the physically interesting case.

Finally in Fig. 3 we see that as  $kz_c$  increases the perturbative range of the phase velocity shrinks near the origin, where  $\omega/k \ll 1$ . This behavior is reasonable as  $\omega$  in this figure is measured in units of  $k$  (or in units of Planck scale) and, in the case of realistic values of  $kz_c \simeq 37$ , the point where we have the breakdown of perturbation theory is expected to be several orders of magnitude smaller than the Planck scale (we will give an estimate of this point in conclusions).

## 4 Wavefunction analysis

### 4.1 Zero mode

In Fig.5 and Fig.6 we have plotted the square of the normalized wave function measured in units of  $k$  ( $k^{-1}\chi_{norm}^2$ ) for several values of the energy  $\omega$ , assuming that the values of the parameters  $\Delta$  and  $kz_c$  are kept fixed. In particular, in Fig.6, we observe that for small energies within the perturbative region of  $\omega$  ( $\omega < \omega_f$ ) the wavefunction of the photon is almost constant. This is expected as in the case of RS-model ( $\delta h = 0$  or  $\Delta = 0$ ) the wavefunction can be obtained analytically and it is constant, see Eq. (36). As the energy of

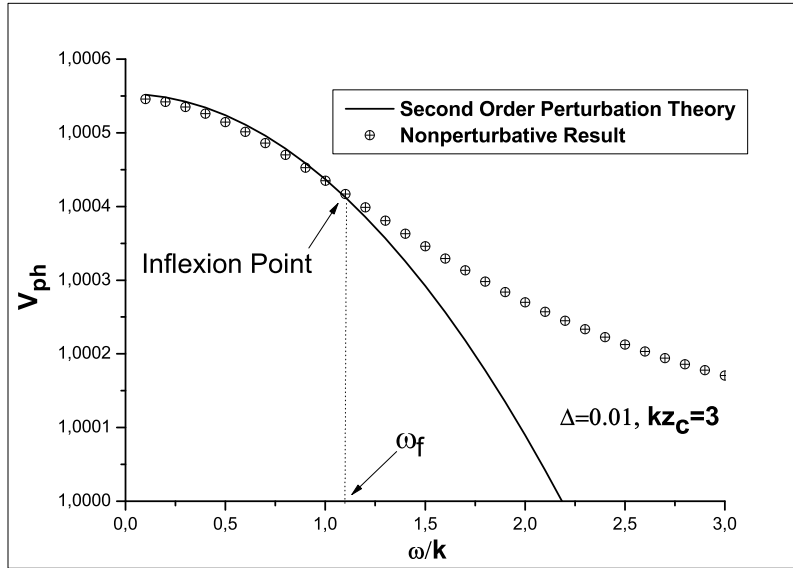


Figure 5: The phase velocity of the photon  $V_{ph}$  as function of  $\omega/k$  for  $kz_c = 3$  and  $\Delta = 0.01$ . The discrete points are the nonperturbative results, and the continuous line corresponds to perturbation theory:  $V_{ph}(\omega) = 1.00055 - 0.00012 (\omega/k)^2$ , where the coefficients have been computed by the formulas of Eqs. (2.30) and (2.31) in Ref. [2]. We see that the inflexion point  $\omega_f \simeq 1.1 k$  separates the perturbative from the nonperturbative sector of the theory.

the photon increases the value of the wave function on the TeV brane ( $\chi_{norm}(z_c)$ ) decreases, see Fig.6. For  $\omega = \omega_f$  the value of the wave function on the TeV brane is half of its value at  $\omega \simeq 0$ , while for larger values of  $\omega$  ( $\omega > \omega_f$ ) it tends rapidly to zero. On the other hand, we see that the wave function on the Planck brane increases. Especially, in Fig. 7 we have plotted the wavefunction of the photon for even larger values of  $\omega$ , deep in the nonperturbative sector of the theory. It seems that the wavefunction on the Planck brane tends to take a limiting value, quite larger than that for  $\omega \simeq 0$ .

If we take into account that the "effective" coupling constant of the zero mode (4D photon), with matter localized on the TeV brane, is proportional to  $\chi_{norm}(kz_c)$  (see [15, 16]), we conclude that photons with very high energies  $\omega \gg \omega_f$  tend to decouple from matter which is localized on the TeV brane. Note, that a similar behavior has been observed for the massive KK modes of the 5D photon, which happens for even larger energies, as we see in the next section. On the other hand, in the case of Planck brane the coupling of the photon with matter increases with the energy, and tends to an asymptotic value.

## 4.2 First KK excitation

In this section we examine the wave function and the group velocity of the first KK mode. In particular, in Fig. 8, we see that the projection of the wave function on the TeV brane decreases as the energy of the 1KK mode increases, and for quite large  $\omega$  the value of the normalized wave function becomes almost zero on the TeV brane. This means that

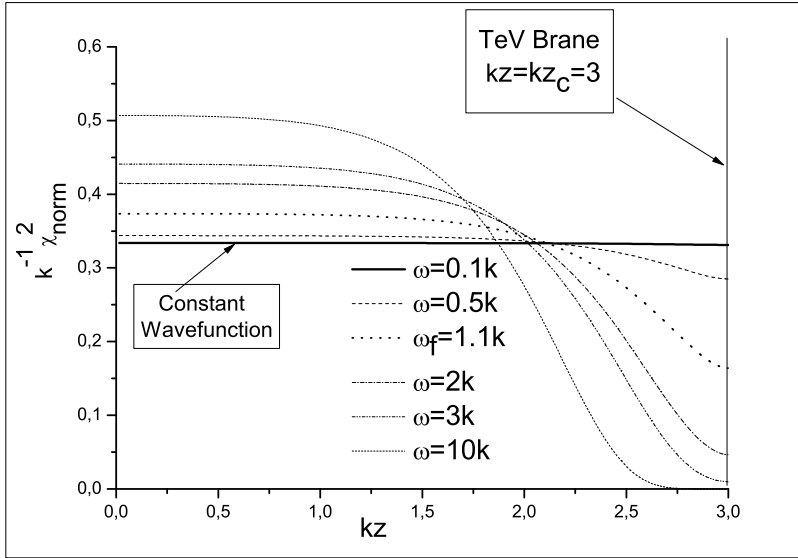


Figure 6: The square of the normalized wave function  $k^{-1}\chi_{norm}^2$  of the zero mode (4D photon) as a function of  $kz$  for  $kzc = 3$ ,  $\Delta = 0.01$  and  $\omega = 0.1k, 0.5k, 1.1k, 2k, 3k, 10k$ . We see that the value of the wave function on the TeV brane (which is proportional to the coupling of the zero mode with the localized matter on the TeV brane) tends to zero as the energy of the zero mode increases. On the other hand, on the Planck brane, we observe that the value of the wave function increases with the energy.

for comparatively large energies where Lorentz violation effects become significant the 1KK mode tends to decouple from matter, which is localized on TeV brane. Note, that a similar behavior was obtained for the zero mode in the previous section. In the case of higher KK excitations a similar behavior is expected. On the other hand the projection of the wave function on the Planck brane is almost constant independently from the energy  $\omega$ .

The 1KK mode is a massive particle, as for zero momentum  $\mathbf{p}$  the energy  $\omega$  takes a nonnegative value  $\omega = m_{1KK} (\neq 0)$ . In Fig. 8, for  $\Delta = 0.01$  and  $kzc = 3$ , we see that  $m_{1KK} = 0.153k$ , as it is the lower energy which is obtained for  $\mathbf{p} = 0$  which corresponds to the inertial mass of the particle. Note that in the case of  $\Delta = 0$ , where we can use the formula

$$m_n^{(0)} = x_n k e^{-kzc}, \quad n = 1, 2, 3, \dots \quad (46)$$

that gives the masses of the KK excitations, where  $x_n$  are the roots of the zeroth order Bessel function  $J_0(x_n) = 0$ . For  $n = 1$  we obtain that  $m_{1KK} = 0.120k$ . However we can use first order perturbation theory to correct this value (see ref. [2]), and now we obtain that  $m_{1KK} = 0.162k$  which is close to the value  $m_{1KK} = 0.153k$  that is obtained nonperturbatively. It is worth noting that in the realistic case  $kzc = 37$  and  $\Delta \sim 10^{-8} \ll 1$  these differences are expected to be more suppressed, and obviously are not detectable in the current high energy experiments, for example in LHC.

As the 1KK mode is a massive particle the phase velocity is not suitable to describe its motion. For this reason in Fig. 9 we have plotted the group velocity of the particle as a

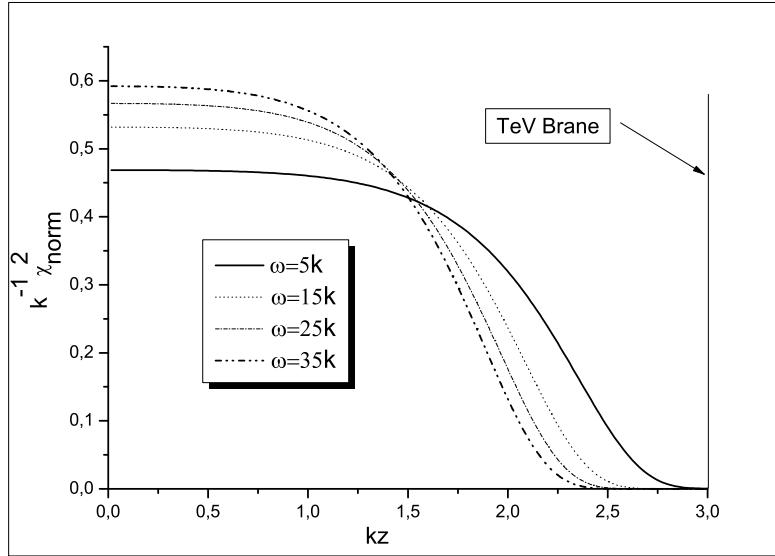


Figure 7: The square of the normalized wave function  $k^{-1}\chi_{norm}^2$  of the zero mode (4D photon) as a function of  $kz$  for  $kz_c = 3$  and  $\Delta = 0.01$  and  $\omega = 5k, 15k, 25k, 35k$ . We observe that the value of the wave function, on the Planck brane, increases with the energy and tends to a constant value.

function of  $\omega/k$ . We see that the energy has a lower bound which characterize the inertial mass of the particle as we have also explained in the previous paragraph. We also see that the group velocity is always smaller than unity, which is the standard velocity of light in the tree level of our model, and tends rapidly to this value  $V_{gr} = 1$  as the energy  $\omega$  increases. Finally, we would like to note that in our model the group velocity of the zero mode, even if it becomes smaller than unity as we see in Fig. 4, is always larger than the group velocity of the first KK mode.

## 5 Discussion

We examined a two brane model where the 5D Lorentz invariance is spontaneously broken due to the nonstandard vacuum of a five-dimensional charged black hole. In this framework we found a mechanism which produces an energy dependent vacuum refractive index, assuming that photons can freely move in the bulk, in contrast to the conventional brane world hypothesis. As perturbation theory was examined extensively in a previous work, in this paper we focused to the nonperturbative case by solving numerically the eigenvalue problem.

We have mainly studied the phase (and the group) velocity of the zero mode, 4D photon, and we found that it is in general a monotonically decreasing function which for very large energies tends to unity, that is the standard velocity of light at tree level of our model. Note that a very similar behavior was obtained for the group velocity of photon, as we can see in Fig. 4 above. On the other hand, in the case of the first KK mode which is a massive particle, we found that the group velocity is always smaller than unity, and it cannot exceed

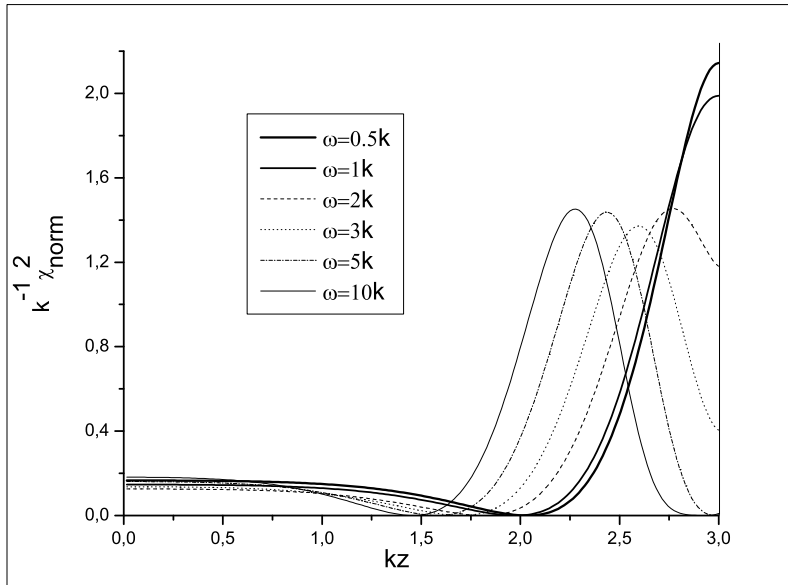


Figure 8: The square of the normalized wave function  $k^{-1}\chi_{norm}^2$  of the 1KK mode as a function of  $kz$  for  $kz_c = 3$  and  $\Delta = 0.01$  and  $\omega = 0.5k, 1k, 2k, 3k, 5k, 10k$ . We see that the value of the wave function on the TeV brane tends to zero as the energy of the 1KK-mode increases. On the other hand, on the Planck brane, we observe that the value of the wave function is almost constant.

the group velocity of the zero mode in the high energy limit.

By comparing with perturbation theory we found that there is an energy  $\omega_f$  after which perturbation theory breaks down. Specifically  $\omega_f$  is the inflection point (see Fig. 5) where the quadratic dependence on energy terminates and the velocity tends to a limiting value. One could give an estimate of this point by comparing with the recent data of the current experiments of MAGIC [17, 18], H.E.S.S [19] and FERMI [20] telescopes. In the case of our model, which predicts a quadratic dependence on the energy for the velocity (see Eq. (2)), the stringent bound is set by the MAGIC experiment:

$$V = 1 - \left( \frac{\omega}{M_2} \right)^2, \quad M_2 \geq 2.6 \times 10^{10} GeV \quad (47)$$

The above restriction was obtained in Ref. [18] by fitting the recent experimental data of MAGIC [17] assuming a quadratic energy dependence for the photon refractive index. Hence, if we take the lowest bound for  $M_2$  ( $M_2 = 2.6 \times 10^{10} GeV$ ) we conclude that the energy  $\omega_f$ , after which perturbation theory breaks down, should be quite smaller than  $2.6 \times 10^{10} GeV$ . Note that the above upper limit, for the inflection point  $\omega_f$ , if it is expressed in eV, gives a value equal to  $2.6 \times 10^{19} eV$  which is close (but smaller) to the energy range of the ultra high energy cosmic rays (particles with astrophysical origin and energies larger than the GZK limit  $7 \times 10^{19} eV$ ). Accordingly the quadratic dependence of velocity of light from the energy  $\omega$ , in the ultra high energy cosmic rays energy region, is not valid any more. Our analysis, in this region of energies, shows that the velocity of light is almost independent from the energy and it has taken a limiting value, which is the velocity of light at tree level of our

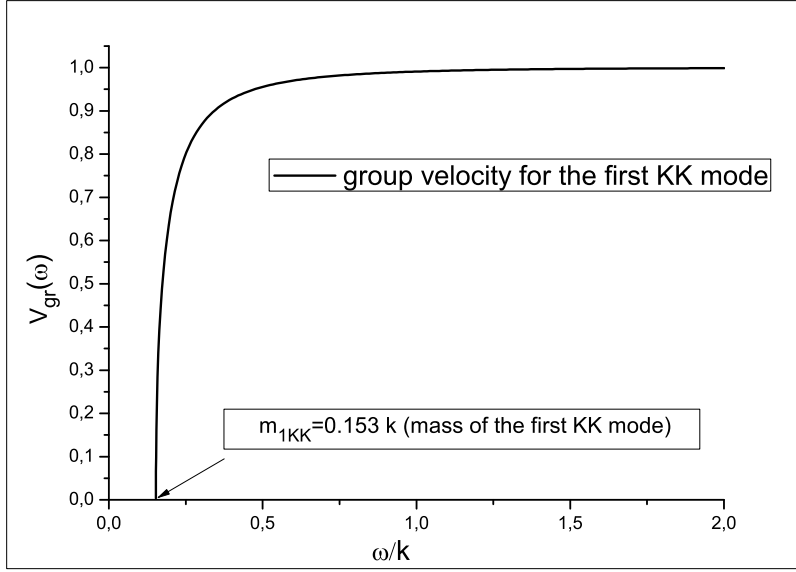


Figure 9: The group velocity  $V_{gr}(\omega)$  as a function of energy in the case of the first KK mode, for  $kz_c = 3$  and  $\Delta = 0.001$ . Note that the group velocity approaches the unity remaining always smaller than the group velocity of the zero mode. We also see in this figure that the energy range has a lower bound which is identified to the mass of the 1KK mode.

model.

In Ref. [21] the authors found the following severe constraint for quadratic dispersion relations:

$$V = 1 - \frac{1}{2}\xi_2 \left( \frac{\omega}{M_{PL}} \right)^2, \quad M_{PL} = 10^{19} GeV, \quad \xi_2 < 2.4 \times 10^{-7}, \quad (48)$$

which is due to the lack of observations of photons above the GZK limit, and appears to be several orders of magnitude stronger than the bounds of MAGIC observations (compare with Eq. (47)). However, this constraint presupposes that the quadratic energy dependence of the velocity of light is valid in the ultra high energy cosmic ray energies, something which does not happen in our model as we have mentioned previously. We conclude that the constraints from the MAGIC observations are the most stringent ones which can be applied to our model.

## Acknowledgements

I would like to thank G. Koutsoumbas, N. Mavromatos and P. Pasipoularides for reading and comment the manuscript. In particular I wish to thank P. Pasipoularides for useful discussions and help with mathematica.

## References

- [1] N. E. Mavromatos, arXiv:0903.0318 [astro-ph.HE].
- [2] K. Farakos, N. E. Mavromatos and P. Pasipoulaides, JHEP **0901** (2009) 057 [arXiv:0807.0870 [hep-th]]; K. Farakos, N. E. Mavromatos and P. Pasipoulaides, arXiv:0902.1243 [hep-th].
- [3] I. Antoniadis, Phys. Lett. B **246** (1990) 377.
- [4] N. Arkani-Hamed, S. Dimopoulos and G. R. Dvali, Phys. Lett. B **429** (1998) 263 [arXiv:hep-ph/9803315].
- [5] I. Antoniadis, N. Arkani-Hamed, S. Dimopoulos and G. R. Dvali, Phys. Lett. B **436**, 257 (1998) [arXiv:hep-ph/9804398].
- [6] L. Randall and R. Sundrum, Phys. Rev. Lett. **83** (1999) 3370 [arXiv:hep-ph/9905221].
- [7] L. Randall and R. Sundrum, Phys. Rev. Lett. **83** (1999) 4690 [arXiv:hep-th/9906064].
- [8] N. E. Mavromatos and E. Papantonopoulos, Phys. Rev. D **73** (2006) 026001 [arXiv:hep-th/0503243].
- [9] N. E. Mavromatos and J. Rizos, Phys. Rev. D **62** (2000) 124004 [arXiv:hep-th/0008074]; N. E. Mavromatos and J. Rizos, Int. J. Mod. Phys. A **18** (2003) 57 [arXiv:hep-th/0205299].
- [10] M. Giovannini, Phys. Rev. D **64** (2001) 124004 [arXiv:hep-th/0107233]; Class. Quant. Grav. **23** (2006) L73 [arXiv:hep-th/0607229]; Phys. Rev. D **75** (2007) 064023 [arXiv:hep-th/0612104]; Phys. Rev. D **75** (2007) 064023 [arXiv:hep-th/0612104]; Phys. Rev. D **76** (2007) 124017 [arXiv:0708.1830 [hep-th]].
- [11] K. Farakos and P. Pasipoulaides, Phys. Lett. B **621** (2005) 224 [arXiv:hep-th/0504014]; K. Farakos and P. Pasipoulaides, Phys. Rev. D **73** (2006) 084012 [arXiv:hep-th/0602200]; K. Farakos and P. Pasipoulaides, Phys. Rev. D **75** (2007) 024018 [arXiv:hep-th/0610010]; K. Farakos, G. Koutsoumbas and P. Pasipoulaides, Phys. Rev. D **76** (2007) 064025 [arXiv:0705.2364 [hep-th]]; P. Pasipoulaides and K. Farakos, J. Phys. Conf. Ser. **68** (2007) 012041.
- [12] C. Csaki, J. Erlich and C. Grojean, Nucl. Phys. B **604** (2001) 312 [arXiv:hep-th/0012143].
- [13] J. M. Cline and H. Firouzjahi, Phys. Rev. D **65** (2002) 043501 [arXiv:hep-th/0107198].
- [14] J. M. Cline and L. Valcarcel, JHEP **0403**, 032 (2004) [arXiv:hep-ph/0312245].
- [15] H. Davoudiasl, J. L. Hewett and T. G. Rizzo, Phys. Lett. B **473** (2000) 43 [arXiv:hep-ph/9911262].
- [16] A. Pomarol, Phys. Lett. B **486** (2000) 153 [arXiv:hep-ph/9911294].

- [17] J. Albert *et al.*, *Astrophys. J.* **669** (2007) 862 [arXiv:astro-ph/0702008].
- [18] J. Albert *et al.* [MAGIC Collaboration] and J. Ellis, N. E. Mavromatos, D. V. Nanopoulos, A. S. Sakharov and E. K. G. Sarkisyan, *Phys. Lett. B* **668** (2008) 253 [arXiv:0708.2889 [astro-ph]].
- [19] F. Aharonian *et al.*, *Phys. Rev. Lett.* **101** (2008) 170402 [arXiv:0810.3475 [astro-ph]].
- [20] A. A. Abdo et al [The Fermi LAT and Fermi GBM collaborations], DOI10.1126/science.1169101 (Science Express Researce Articles), published online 19 February 2009.
- [21] M. Galaverni and G. Sigl, *Phys. Rev. D* **78**, 063003 (2008) [arXiv:0807.1210 [astro-ph]].